Available at www.sciencedirect.com

ScienceDirect

journal homepage: www.elsevier.com/locate/he

An experimental and numerical study on characteristics of laminar premixed H_2/CO/CH_4/air flames

T.S. Cheng [a,*], Y.-C. Chang [b], Y.-C. Chao [b], G.-B. Chen [c], Y.-H. Li [b], C.-Y. Wu [d]

[a] Department of Mechanical Engineering, Chung Hua University, 707, Sec. 2, Wufu Rd., Hsinchu 300, Taiwan, ROC
[b] Department of Aeronautics and Astronautics, National Cheng Kung University, Tainan 701, Taiwan, ROC
[c] Research Center for Energy Technology and Strategy, National Cheng Kung University, Tainan 701, Taiwan, ROC
[d] Department of Electro-Optical Science and Engineering, Kao Yuan University, Kaohsiung County 821, Taiwan, ROC

ARTICLE INFO

Article history:
Received 27 May 2011
Received in revised form
15 July 2011
Accepted 17 July 2011
Available online 26 August 2011

Keywords:
Gasified biomass
Premixed opposed-jet flames
Laminar burning velocity
Chemical kinetic structure

ABSTRACT

The effects of variations in the fuel composition on the characteristics of H_2/CO/CH_4/air flames of gasified biomass are investigated experimentally and numerically. Experimental measurements and numerical simulations of the flame front position and temperature are performed in the premixed *stoichiometric* H_2/CO/CH_4/air opposed-jet flames with various H_2 and CO contents in the fuel. The adiabatic flame temperatures and laminar burning velocities are calculated using the EQUIL and PREMIX codes of Chemkin collection 3.5, respectively. Whereas the flame structures of the laminar premixed stoichiometric H_2/CO/CH_4/air opposed-jet flames are simulated using the OPPDIF package with the GRI-Mech 3.0 chemical kinetic mechanisms and detailed transport properties. The measured flame front position and temperature of the stoichiometric H_2/CO/CH_4/air opposed-jet flames are closely predicted by the numerical calculations. Detailed analysis of the calculated chemical kinetic structures reveals that the reaction rate of reactions (R38), (R46), and (R84) increase with increasing H_2 content in the fuel mixture. It is also found that the increase in the laminar flame speed with H_2 addition is most likely due to an increase in active radicals during combustion (chemical effect), rather than from changes in the adiabatic flame temperature (thermal effect). Chemical kinetic structure and sensitivity analyses indicate that for the stoichiometric H_2/CO/CH_4/air flames with fixed H_2 concentration in the fuel mixture, the reactions (R99) and (R46) play a dominant role in affecting the laminar burning velocity as the CO content in the fuel is increased.

1. Introduction

Extensive fossil fuel consumptions have resulted in rapid gasoline depletion as well as atmospheric and environmental pollutions. In order to alleviate these impacts, two alternative strategies are currently considered: either to improve the combustion efficiency with considerable reductions in the pollutant emissions into the atmosphere or more significantly, to replace fossil fuel utilization as much as possible with environmentally friendly, clean and renewable energy sources [1]. Among the various renewable energy sources, the use of gasified biomass can be more versatile and attractive due to its wide availability, reduction of CO_2 emission, and contribution to diversification of energy supply and rural development. It becomes essential, therefore, to develop combustion techniques that can burn the gasified biomass or

* *Corresponding author*. Tel.: +886 3 518 6489; fax: +886 3 518 6521.
E-mail address: tscheng@chu.edu.tw (T.S. Cheng).

0360-3199/$ – see front matter
doi:10.1016/j.ijhydene.2011.07.077

low-grade syngas effectively and to understand chemical and physical properties of flames for such kind of fuels.

For the majority of gasified biomass, it contains typically a mixture of CO (17–40%), H_2 (4–32%), CH_4 (3–10%), CO_2 (15–36%) and N_2 (50–65%), all on volumetric basis [2–4]. The considerable variations in the composition of gasified biomass depend upon various biomass sources and processing techniques. The purification of gasified biomass can be made by removing CO_2 and N_2 using pressure swing adsorption, amine scrubbing and membrane reactors. Since the combustion characteristics of biomass (blended) fuels may differ substantially from those of single-component fuels, therefore, detailed investigation and in-depth understanding of the gasified biomass combustion characteristics, such as laminar burning velocity, flame structure, and chemical kinetics, are of vital importance. Laminar burning velocity is an important parameter of a combustible mixture as it contains fundamental information on reactivity, diffusivity, and exothermicity. Yu et al. [5] investigated the laminar burning velocity of CH_4–H_2 mixtures and found that the laminar burning velocities increase linearly with increasing hydrogen fraction in the fuel blends. Halter et al. [6] investigated the effect of initial pressure and hydrogen fraction on the laminar burning velocity of CH_4–H_2 flame and their results showed that the laminar burning velocity increases with increasing hydrogen fraction in fuel blends and deceases with increasing the initial pressure. Recently, the effects of H_2 addition on laminar burning velocity, flame temperature, and flame stability of CH_4–H_2–air flames [7–9] and natural gas-hydrogen-air flames [10] were also extensively investigated. These studies indicate that the increase of H_2 addition enhances the flame temperature and laminar burning velocity but decreases the Markstein length. In addition, the laminar burning velocity of four biomass derived gases was experimentally measured and compared to numerical predictions using GRI-Mech 2.11 and 3.0 mechanisms [11].

The combustion characteristics of CO, which is a major species in the gas mixture of gasified biomass, are different from those of H_2 and other alkanes. Its combustion can be characterized by dry oxidation, i.e. $CO + O_2 \rightarrow CO_2 + O$. However, in practical combustion processes, the oxidation of CO can be significantly accelerated by the reaction $CO + OH \leftrightarrow CO_2 + H$ when there is a small amount of hydrogen-containing species in the fuel or oxidizer stream [12]. The burning velocity of CO with hydrogen-containing species liberated from hydrogen, alkanes, or even water vapor is several times higher than that of dry oxidation [13]. The effect of small quantities of hydrocarbon addition on the kinetics of $CO/H_2O/O_2$ mixtures was investigated by Yetter and Dryer [14] in homogenous, low- to intermediate-temperature flow reactors. The effects of CO_2 addition on the extinction and NO_x emission characteristics of $H_2/CO/CO_2$ syngas mixtures were reported by Park et al. [15] and Ouimette and Seers [16], respectively. Park et al. [15] found that chemical effects of added CO_2 reduce critical CO_2 mole fraction at flame extinction and thus extinguish the flame at higher flame temperature irrespective of global strain rate. Ouimette and Seers [16] reported that the addition of CO_2 to syngas fuel decreases flame temperature, flame height, and NO_x emission. Moreover, the effect of N_2 and CO_2 dilutions on the laminar burning velocity and Markstein length of dissociated methanol-air mixtures was experimentally studied by Zhang et al. [17]. The effect of H_2 and CH_4 additions on the propagation and extinction of atmospheric CO/air opposed-jet flames was experimentally and numerically studied by Vagelopoulos and Egolfopoulos [18]. They found that the addition of small amounts of H_2 or CH_4 to CO flames increases the laminar flame speeds and extinction strain rates by accelerating the main CO oxidation reaction. In the previous research, the authors experimentally and numerically investigated the effects of CO addition on the characteristics of laminar premixed CH_4/air opposed-jet flames [19]. We found that as the CO content in the fuel is increased from 0% to 80%, CO oxidation increases significantly and contributes to a significant level of heat-release rate. In addition, the laminar burning velocity reaches a maximum value (57.5 cm/s) at the condition of 80% of CO in the fuel. The chemistry of CO consumption shifts to the dry oxidation kinetics when CO content is further increased over 80%. The effect of CO addition on the laminar burning velocity of the stoichiometric CH_4/CO/air flames is due mostly to the transition of the dominant chemical kinetic paths.

Since CO and H_2 are also the intermediate species of hydrocarbon flames, the intrinsic interaction between the original CO and H_2 in the fuel blend and those produced from oxidization of hydrocarbons and the effects of such interaction on flame characteristics are still not clear. Moreover, a literature survey indicates that systematic investigations, especially on the laminar burning velocities, flame structures, and the transition of chemical reactions in flames of the H_2/CO/CH_4 blended fuels are still deficient. Hence, a better understanding of the detailed combustion characteristics of $H_2/CO/CH_4$ blended fuels is warranted not only from a fundamental point of view but also for practical applications. This motivates the present study to systematically investigate the laminar premixed $H_2/CO/CH_4$/air flames and their reaction characteristics, through experimental measurements and numerical simulations of the opposed-jet flames, which have been widely employed in previous fundamental studies [18–21]. In the present study, the laminar burning velocities and adiabatic flame temperatures of the *stoichiometric* $H_2/CO/CH_4$/air flames under various fuel compositions are firstly calculated to understand the effects of fuel mixture variations on the propagation and exothermicity of the flames. In addition, the flame front position and temperature of the premixed stoichiometric $H_2/CO/CH_4$/air opposed-jet flames under various fuel compositions are measured and compared with numerical predictions to examine the effects of blended fuel variations on the flame structure and chemical characteristics. Finally, the calculated chemical kinetic structures for some selected flames are compared and the key reactions that affect the flame structure, heat-release rate, and laminar flame speed are discussed.

2. Methods of investigation

2.1. *Experimental methods*

The experimental setup is schematically shown in Fig. 1. The opposed-jet burner consists of two water-cooled, well-

contoured circular nozzles (i.d. = 2 cm) with slow coaxial shielding flows. Two premixed H_2/CO/CH_4/air jets are directed toward each other to form two symmetrical, planar flames at atmospheric pressure condition. Both premixed flames are operated at the fixed stoichiometric condition while the volumetric concentration of H_2, CO, and CH_4 are varied in the blended fuel. The separation distance between two nozzles is 2 cm and the bulk velocity at each jet exit is maintained at 2 m/s (global strain rate = 200 s^{-1}) for the present study. Research-grade fuels and compressed air are metered by electronic mass flowmeters and mixed in a mixing chamber prior to the opposed-jet burner. The flame is shielded from ambient air by a nitrogen coaxial flow with low velocity, which is controlled using a rotameter. The experimental conditions of the premixed stoichiometric H_2/CO/CH_4/air opposed-jet flames are listed in Table 1. In experiments, the visible flame features are obtained using a high sensitivity 3-chip color CCD camera (Sony DXC-9000) and digitized by the frame grabber for further digital image processing to identify the flame front position. An R-type (Pt/Pt-13Rh) thermocouple with 25 μm wire diameter is used to measure the flame temperature. BeO and 10–15% Y_2O_3 coating is applied to eliminate catalytic reactions induced by platinum in the flame [22]. The measured temperature in the flame is corrected for radiation heat loss by assuming a spherical thermocouple bead [23,24].

2.2. Numerical methods

The adiabatic flame temperatures and free propagation velocities of the premixed stoichiometric H_2/CO/CH_4/air flames are calculated using the EQUIL and PREMIX codes of Chemkin collection 3.5, respectively. Whereas the flame structures of the laminar premixed stoichiometric H_2/CO/CH_4/air opposed-jet flames are simulated using the OPPDIF package with the GRI-Mech 3.0 full chemical kinetic mechanism [25] and detailed transport properties. The initial temperature and pressure for all calculations made in the present study are 300 K and 1 atm, respectively. For the opposed-jet flame calculations, the computation domain and input parameters for each flame condition are in accordance with experiments. In flowfield computation, the flow is reduced mathematically to one dimension by assuming that the radial velocity varies linearly in the radial direction, which leads to a simplified form in which the flowfield properties are functions of the axial distance only. The adaptive re-gridding method is applied to solve the flame structure, and the grid independence of the solutions is achieved by tuning the GRAD and CURV parameters in the package. The number of grid lines is more than 400 for each case. The minimum grid dimension is approximately 0.1 μm, which is sufficient to resolve the flame thickness and the steep temperature gradient.

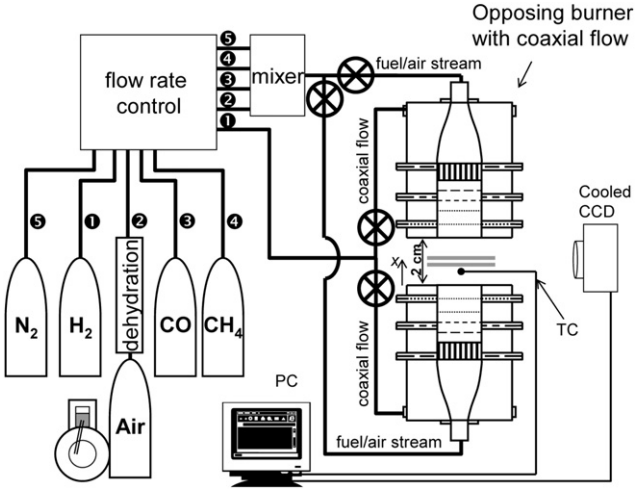

Fig. 1 – Experimental apparatus of the fuel supply system and opposed-jet burner.

3. Results and discussion

3.1. Adiabatic flame temperature and laminar burning velocity

In order to investigate the effect of fuel composition variations on the characteristics of blended fuel combustion, the attention is focused on *stoichiometric* flames. The effect of fuel composition variations on the adiabatic flame temperatures of premixed stoichiometric H_2/CO/CH_4/air flames is shown in Fig. 2. It can be seen that when there is no CO in the fuel mixture, the adiabatic flame temperature increases only 10 K with 20% of H_2 addition to the CH_4/air flame and another 24 K increase when H_2 volumetric fraction is increased from 20% to 50%. The results indicate that the addition of H_2 to the CH_4/air flame has a little effect on flame temperature. This finding is in good agreement with that reported by Wang et al. [8]. When

Table 1 – Experimental conditions of the premixed stoichiometric H_2/CH_4/CO/air opposed-jet flames.

Flame No.	H_2/CO/CH_4 Fuel mixture (vol %)			CO/CH_4 Fuel mixture (vol %)		Air (vol %)
	H_2	CO	CH_4	CO	CH_4	
1	0	10	90	10	90	89.8
2	0	50	50	50	50	85.61
3	0	80	20	80	20	79.2
4	0	98	2	98	2	71.61
5	10	0	90	0	100	89.80
6	10	9	81	10	90	89.09
7	10	45	45	50	50	84.83
8	10	72	18	80	20	78.56
9	10	76.5	13.5	85	15	76.98
10	10	81	9	90	10	75.14
11	10	84.6	5.4	94	6	73.44
12	10	88.2	1.8	98	2	71.50
13	10	90	0	100	0	70.41
14	20	0	80	0	100	89.00
15	20	8	72	10	90	88.26
16	20	40	40	50	50	83.96
17	20	64	16	80	20	77.89
18	20	68	12	85	15	76.40
19	20	72	8	90	10	74.69
20	20	75.2	4.8	94	6	73.14
21	20	78.4	1.6	98	2	71.38
22	20	80	0	100	0	70.41

there is no H_2 in the fuel mixture, the adiabatic flame temperature increases only 12 K with 20% of CO addition to the CH_4/air flame and another 27 K increase when CO is increased from 20% to 50%. Further increase of CO from 50% to 100% increases flame temperature by 119 K. This fact suggests that the addition of CO to the CH_4/air flame has a slightly larger effect on flame temperature than that of H_2. For the stoichiometric H_2/CO/CH_4/air flame, the adiabatic flame temperature increases with increasing H_2 and CO concentrations in the fuel mixture. However, the addition of H_2 does not significantly change the adiabatic flame temperature when CO concentration in CO/CH_4 fuel mixture reaches 94%. The adiabatic flame temperature reaches a maximum value when CO in CO/CH_4 fuel mixture is increased to 100%. For the stoichiometric H_2/CO/air syngas flame, the increase of H_2 concentration from 0% to 50% decreases the adiabatic flame temperature from 2385 K to 2371 K. Computed results suggest that at stoichiometric condition the addition of CO has more effect on the adiabatic flame temperature than that of H_2.

The computed laminar burning velocities of the premixed stoichiometric H_2/CH_4/CO/air flames under various H_2/CO/CH_4 fuel compositions are shown in Fig. 3. Note that the laminar burning velocity is calculated based on the "dry" oxidation condition, i.e., no water vapor is present in the air. Fig. 3 shows that when there is no CO in the fuel mixture, the laminar burning velocity increases with increasing H_2 addition to the CH_4/air flame. The increase of H_2 volumetric fraction from 0% to 50% increases the laminar burning velocity from 38 cm/s to 57 cm/s. It can also be seen that with 0% of H_2 in the fuel mixture, the laminar burning velocity increases with increasing CO content in the CH_4/air flame, and it reaches a maximum value (55.5 cm/s) at the condition of 80% of CO in fuel and decreases rapidly as CO is further increased. As the concentration of CO is higher than 80%, due to insufficient

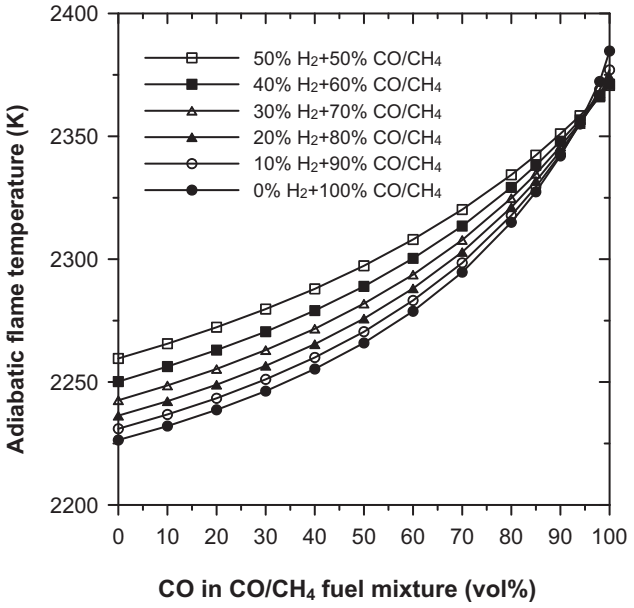

Fig. 2 – Computed adiabatic flame temperature of the stoichiometric H_2/CO/CH_4/air flames as a function of CO contents in the CO/CH_4 fuel mixture with various H_2 additions.

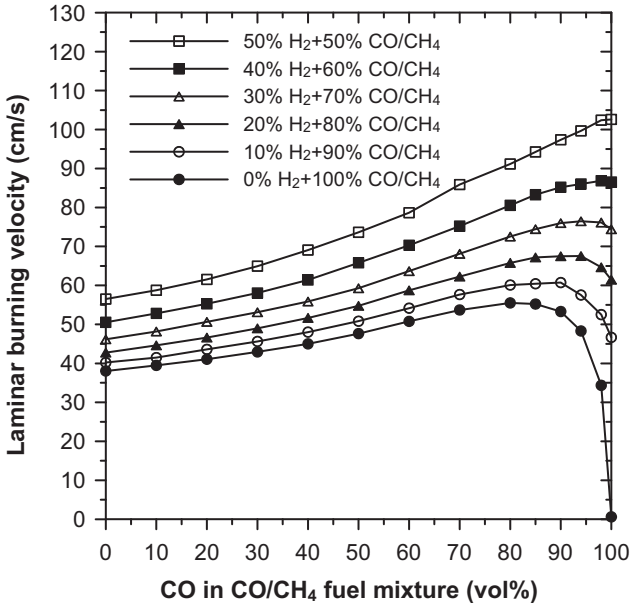

Fig. 3 – Computed laminar burning velocity of the stoichiometric H_2/CO/CH_4/air flames as a function of CO contents in the CO/CH_4 fuel mixture with various H_2 additions.

H atom in flame, the oxidation of CO is dominated by dry oxidation step (R12) which has a lower heat release rate and leads to a slower reaction. This suggests that the insufficient amount of H atom, due to the limited amount of CH_4 in the fuel, decelerates the reaction of (R99), generates less heat release and hence results in a significantly decrease of laminar burning velocity [19]. When 10% of H_2 is added to the CO/CH_4 fuel mixture, the laminar burning velocity is increased, especially for the condition of 100% of CO in the CO/CH_4 mixture. Note that the burning velocity has increased from near zero (0.608 cm/s) for the pure CO flame to a value of 46 cm/s for the 10% H_2-90% CO-0% CH_4 (100% CO in CO/CH_4) flame. In addition, the increase of H_2 content in the blended fuel not only increases the burning velocity, but also shifts the maximum burning velocity from that occurred at the condition of 10% H_2-81% CO-9% CH_4 (90% CO in CO/CH_4) to 50% H_2-50% CO-0% CH_4 (100% CO in CO/CH_4). Comparison of Figs. 2 and 3 indicates that the adiabatic flame temperature and laminar burning velocity of the stoichiometric H_2/CH_4/CO/air flames are influenced not only by the content of H_2, but also by the CO concentration in the fuel mixture. This fact suggests that further investigations of the flame and chemical kinetic structures of the premixed stoichiometric H_2/CO/CH_4/air flames are needed.

3.2. *Flame appearance and flame front position*

Photographs of the premixed stoichiometric H_2/CO/CH_4/air opposed-jet flames with 10% and 20% of H_2 and various CO contents in the CO/CH_4 mixture are shown in Fig. 4. Note that the flame appearances of the CO/CH_4/air opposed-jet flames (global strain rate = 100 s^{-1}) were reported previously [19]. Moreover, in the present study the maximum addition of H_2 is

maintained below 20% to avoid the flame standing too close to the burner exit that could damage the burner. When 10% and 20% of H_2 are added to the CO/CH_4 mixture, the overall flame appearances are similar to those of CO/CH_4/air flames except for the case of 100% CO in CO/CH_4 mixture. For the pure CO premixed flame, the two symmetrical, planar flames almost merge into a single flame and the flame becomes silver-white in color in the center and blue near the edge of the flame [19]. Fig. 4 shows that at low CO concentrations (≤10%), two symmetrical, planar flames exist and the flames are blue in color. As the CO concentration is increased, the postflame zone (region between two planar flames) immediately becomes orange in color and extends in lateral direction. It is noted that the separation distance between two symmetrical flames increases with increasing CO concentration. The separation distance reaches a maximum value at the conditions of 90% CO and 94% CO in CO/CH_4 for 10% and 20% of H_2 additions, respectively. Fig. 4 also indicates that the increase of H_2 addition to the CO/CH_4/air mixtures increases the separation distance and changes the flame front position.

In order to determine the flame front position, direct photographs of the premixed stoichiometric $H_2/CO/CH_4$/air opposed-jet flames are performed. The flame front position (the distance from the nozzle exit) is determined at the location along the jet axis where maximum flame luminosity occurs. Comparison of the measured and predicted flame front positions is shown in Fig. 5 to examine the effects of H_2 and CO contents on the flame structure and to validate the numerical predictions. For the opposed-jet flames, the calculated flame front position is defined at the axial location of maximum temperature gradient. Fig. 5 shows the good agreements between the measured and predicted results. It can be seen that for 10% and 20% of H_2 additions the flame front position decreases with increasing CO concentration. It reaches a minimum value at 90% and 94% of CO in the CO/CH_4 fuel for 10% and 20% of H_2 additions respectively and then increases as CO is further increased. It is interesting to note that the profile of the variation of flame front position with CO contents in the $H_2/CO/CH_4$/air mixtures looks like an inversion

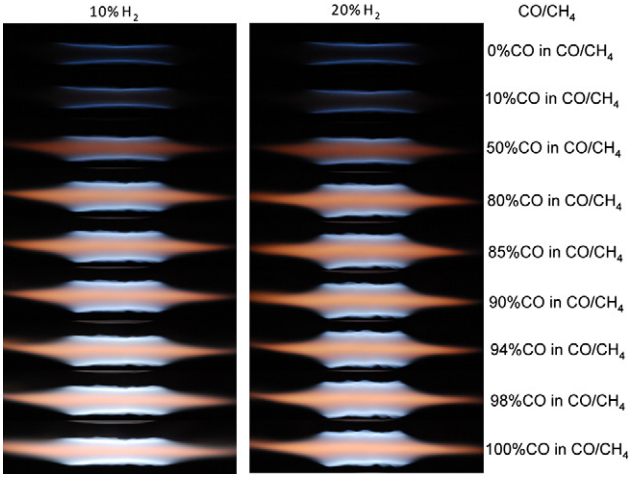

Fig. 4 – Photographs of the premixed stoichiometric $H_2/CO/CH_4$/air flames with 10% and 20% H_2 additions and various CO contents in the CO/CH_4 fuel mixture.

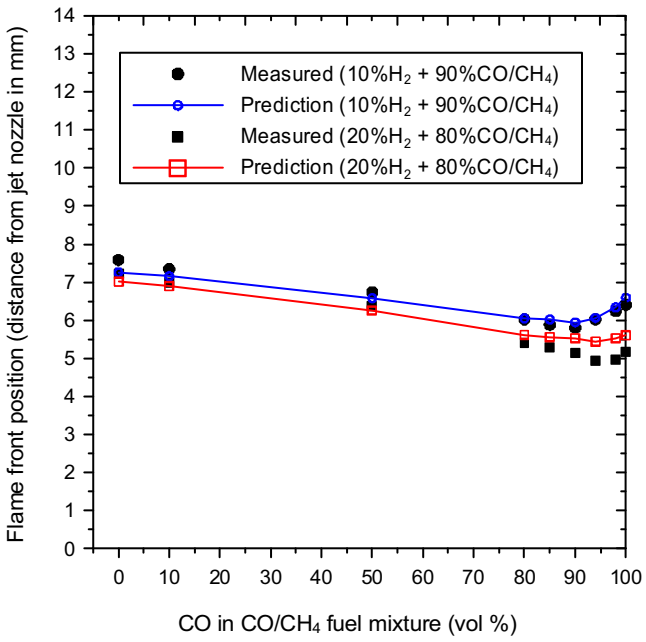

Fig. 5 – Comparison of the measured and calculated flame front positions for the premixed stoichiometric $H_2/CO/CH_4$/air flames.

of the laminar burning velocity profile (Fig. 3). Comparison of Figs. 3 and 5 indicates that flame 10 (10% H_2-81% CO-9% CH_4) and flame 20 (20% H_2-75.2% CO-4.8% CH_4) have the maximum laminar burning velocity and produce the shortest distance from the nozzle to the flame front position as compared to other flame cases studied. The effects of H_2 and CO variations on the flame speed and flame front position are closely related to the chemical kinetics of the blended fuels.

3.3. *Temperature measurement*

In addition to measurements of the flame front position for premixed stoichiometric $H_2/CO/CH_4$/air opposed-jet flames, temperature measurements are also performed. Typical results for 0%, 10%, and 20% of H_2 additions with various CO and CH_4 contents coupled with numerical predictions of temperature are shown in Fig. 6. For temperature measurements, only the preheated and partial oxidation zones are measured due to the limitation of the R-type thermocouple (~2040 K). Fig. 6 shows that for 0% of H_2 addition, four flames result in a similar temperature gradient, but the preheat zone for the 80% CO-20% CH_4 flame shifts closest to the nozzle exit and leads to a slightly higher calculated flame temperature. When 10% and 20% of H_2 are added to the fuel mixture, the preheated zone closest to the nozzle exit occurs at the condition of flame 10 (10% H_2-81% CO-9% CH_4) and flame 20 (20% H_2-75.2% CO-4.8% CH_4), respectively. The predicted flame temperatures are in good agreement with the measured data for all the flames measured. Comparisons of the predicted flame front position and temperature with the measured data indicate that the numerical model can accurately predict the general flame characteristics. This, in turn, validates the correct settings of the boundary conditions in the model and

also shows the capability of the combustion model and mechanism used for the current H_2/CO/CH_4/air flame calculations. This fact suggests that the model can be used for further analysis of the flame chemical structures as the composition of the blended fuel is varied.

3.4. *Effect of H_2 addition on chemical kinetic structures*

In order to understand the effects of H_2 addition on flame characteristics, detailed flame structures for 0%, 10%, and 20% of H_2 additions with fixed CO/CH_4 volumetric ratio at 4/1 are examined. The profiles of the temperature, species mole fraction, production rate, net reaction rate, and heat-release rate of the major elementary steps along the jet axis are plotted in Figs. 7, 8 and 9 for flames 3, 8, and 17, respectively. In the figures the dashed line indicates the axial location of the peak temperature gradient which separates the preheat zone and the oxidation zone. Fig. 7 shows the calculated chemical

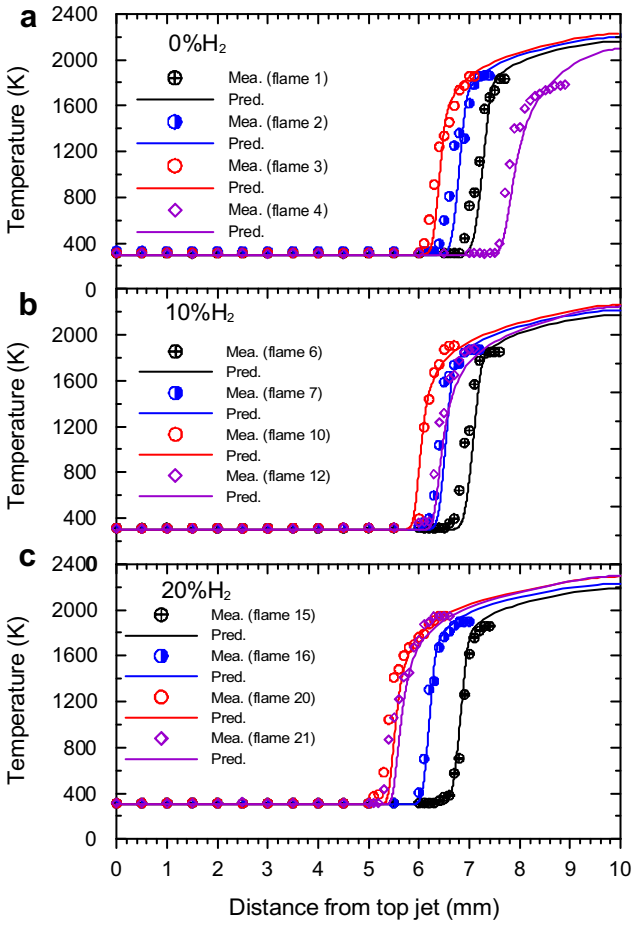

Fig. 6 – Comparison of the measured and calculated flame temperatures for the premixed stoichiometric H_2/CO/CH_4/air flames: flame 1 (0% H_2-0% CO-90% CH_4), flame 2 (0% H_2-50% CO-50% CH_4), flame 3 (0% H_2-80% CO-20% CH_4), flame 4 (0% H_2-98% CO-2% CH_4), flame 6 (10% H_2-9% CO-81% CH_4), flame 7 (10% H_2-45% CO-45% CH_4), flame 10 (10% H_2-81% CO-9% CH_4), flame 12 (10% H_2-88.2% CO-1.8% CH_4), flame 15 (20% H_2-8% CO-72% CH_4), flame 16 (20% H_2-40% CO-40% CH_4), flame 20 (20% H_2-75.2% CO-4.8% CH_4), flame 21 (20% H_2-78.4% CO-1.6% CH_4).

structures for 0% H_2-80% CO-20% CH_4 flame which are similar to those previously reported in [19] except that higher global strain rate is employed in the present study. The distributions of temperature, species mole fraction, and production rate, shown in Fig. 7a and b, are similar to premixed stoichiometric methane flame except the existence of CO in the preheat zone. It can be seen that the CO is decreasing gradually due to the accompanied production of the intermediate CO from methane oxidation. Fig. 7c and d show the net reaction rate and the heat-release rate of major elementary steps. It can be seen from Fig. 7c that the most significant reaction is the chain-branching reaction $H + O_2 \leftrightarrow OH + O$ (R38) followed by the oxidation of CO through reaction $OH + CO \leftrightarrow H + CO_2$ (R99). In the preheat zone, the rate of reaction $HO_2 + H \leftrightarrow OH + OH$ (R46) for OH production and the rate of reaction (R99) for CO oxidation exceed that of reactions $OH + CH_4 \leftrightarrow CH_3 + H_2O$ (R98) and $H + CH_4 \leftrightarrow CH_3 + H_2$ (R53) for the dehydrogenation of methane, and the reaction (R98) occurs slightly prior to the reaction (R53). Therefore, in the preheat zone, the OH radicals react with CO through a faster reaction rate compared to that of methane oxidation and hence, results in a faster CO consumption rate (Fig. 7b). In the oxidation zone, the production of the intermediate CO is mainly from the reactions $O + CH_3 \rightarrow H + H_2 + CO$ (R284) and $O_2 + HCO \leftrightarrow HO_2 + CO$ (R168). The large amount of OH produced from reaction (R38) is mainly for CO oxidation reaction (R99) and to form the product H_2O as well as to further build up the H radical pool through reaction $OH + H_2 \leftrightarrow H + H_2O$ (R84), though the dehydrogenation of methane through reaction (R98) is still very active. Thus the reaction (R99) almost dominates the overall reaction rate (Fig. 7c) and contributes most of the positive heat release in the preheated and oxidation zones (Fig. 7d). Fig. 7d indicates that the major contributions to the positive heat release are the reactions, including $O + CH_3 \leftrightarrow H + CH_2O$ (R10), $OH + CO \leftrightarrow H + CO_2$ (R99), $O + CH_3 \rightarrow H + H_2 + CO$ (R284), $HO_2 + H \leftrightarrow OH + OH$ (R46), $O_2 + HCO \leftrightarrow HO_2 + CO$ (R168), $OH + H_2 \leftrightarrow H + H_2O$ (R84), $OH + CH_4 \leftrightarrow CH_3 + H_2O$ (R98), $OH + CH_2O \leftrightarrow HCO + H_2O$ (R101), and $H + CH_2O \leftrightarrow H_2 + HCO$ (R58). The major negative contributors are (R38) and (R167). The major reaction steps discussed in this paper are summarized in Table 2.

Fig. 8 shows the calculated axial variations of variables for flame 8 (10% H_2-72% CO-18% CH_4). It is noted that although the volumetric fraction of CO and CH_4 is varied, the CO/CH_4 volumetric ratio is remained constant at 4/1 so that the effect of H_2 addition on flame characteristics can be examined. As 10% of H_2 is added to the fuel mixture, several noticeable features are observed. Fig. 8a shows that the decrease of H_2 mole fraction becomes larger and occurs earlier than that of CO and CH_4 in the preheat zone. This could be due to the fact that the initiation reaction of H_2 is faster than that of CO and CH_4, and its original concentration (10%) is lower than CO (72%) and CH_4 (18%) in the fuel mixture. In the oxidation zone, however, its oxidation rate is reduced due to accompanied production of the intermediate H_2 from methane oxidation. It can be seen from Fig. 8c that the addition of H_2 in the fuel mixture not only increases the rate of reactions (R38) and (R46) to produce more OH radicals, but also accelerates the rate of H_2 oxidation through reaction (R84) to further build up the H

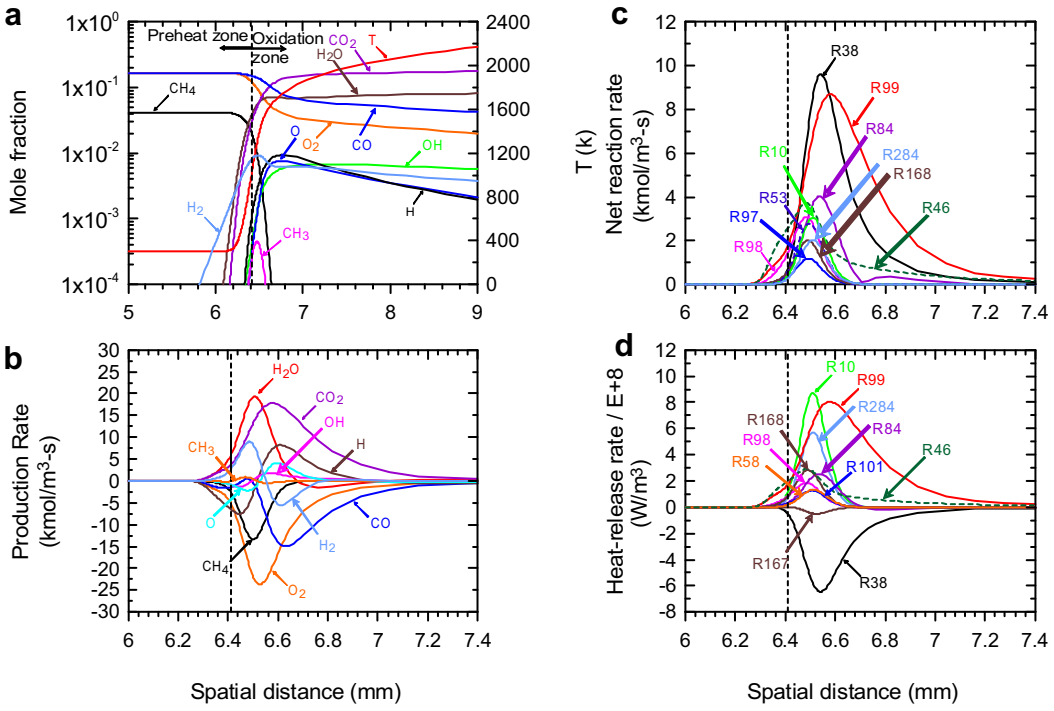

Fig. 7 – Computed axial distributions of temperature, species mole fraction, production rate, net reaction rate and heat-release rate for flame 3 (0% H_2-80% CO-20% CH_4).

radical pool, as compared to Fig. 7c. Although the additive H_2 enhances the rate of reaction (R84), its reaction rate, however, is still less than the rate of CO oxidation (R99). Thus the CO oxidation reaction (R99) still dominates the overall reaction rate and contributes most of the positive heat release in the preheated and oxidation zones (Fig. 8d).

As the concentration of H_2 is further increased to 20%, the calculated axial distribution of variables is shown in Fig. 9 for flame 17 (20% H_2-64% CO-16% CH_4). For such an amount of additive H_2 in the fuel mixture, its chemistry plays an equivalent role with CO in the overall reaction as evident by the consumption rates of H_2 and CO (Fig. 9b). Fig. 9c also shows

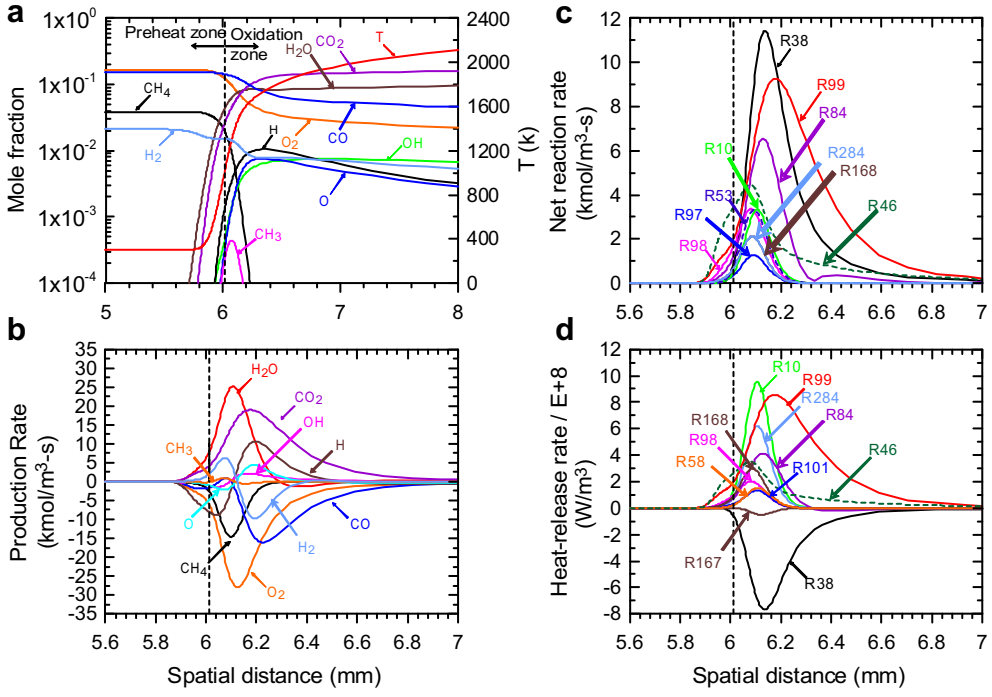

Fig. 8 – Computed axial distributions of temperature, species mole fraction, production rate, net reaction rate and heat-release rate for flame 8 (10% H_2-72% CO-18% CH_4).

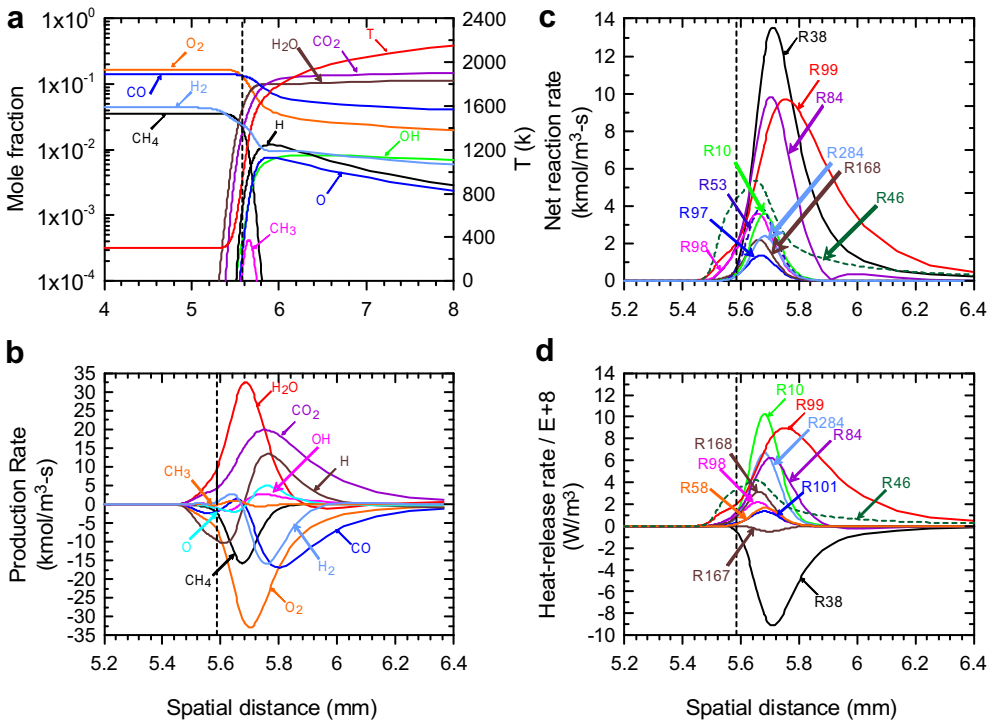

Fig. 9 – Computed axial distributions of temperature, species mole fraction, production rate, net reaction rate and heat-release rate for flame 17 (20% H_2-64% CO-16% CH_4).

that the rate of H_2 oxidation reaction (R84) is comparable to that of CO oxidation reaction (R99) except that the reaction (R99) extends broader than reaction (R84) in the oxidation zone. The rate of methane dehydrogenation reactions (R98) and (R53) is less than the rate of OH production reactions (R38) and (R46). The produced OH radicals accelerate the H_2 and CO oxidations through reactions (R84) and (R99) which contribute to most of heat release in this flame.

Comparison of the computed chemical kinetic structures (Figs. 7–9) reveals that for a fixed stoichiometry of the H_2/CO/CH_4/air flame with H_2 content ranging from 0% to 20%, the reaction rate of reactions (R38), (R46), and (R84) increase with increasing H_2 content in the fuel mixture. The increase of the rate of reactions (R38) and (R46) enhances active OH radical productions, while the increase of the rate of reaction (R84) accelerates H_2 oxidation. The reaction (R38) contributes to negative heat release and the reactions (R46) and (R84), although they contribute to positive heat release, only release a small amount of heat as compared to other major reactions. These facts suggest that the increase in the laminar flame speed (see Fig. 3) with H_2 addition to stoichiometric H_2/CO/CH_4/air flame is most likely due to an increase in active radicals during combustion (chemical effect), rather than from changes in the adiabatic flame temperature (thermal effect). This finding is in good agreement with that reported by Sung et al. [26] for the H_2 addition to n-butane/air mixture.

3.5. *Effect of CO variation on chemical kinetic structures*

In order to further understand the effects of CO and CH_4 variations on flame characteristics, the calculated net reaction rate and heat-release rate are illustrated in Figs. 10 and 11, respectively, for five selected flames with H_2 concentration fixed at 20%. It is noted that the volumetric fraction of CO is varied from 8% to 78.4%, while the CH_4 concentration is also changed accordingly to keep the CO–CH_4 total concentration at 80%. It can be seen from Fig. 10 that when CO concentration in the fuel mixture is low (8%), the overall reaction is dominated by both H_2 through reaction (R84) and CH_4 through reactions (R53) and (R98). As CO concentration is increased to the same amount as the CH_4 (40%), the rates of reactions (R99)

Table 2 – Summary of the major reaction steps.

Reaction number	Reaction step
(R3)	$O + H_2 \leftrightarrow OH + H$
(R10)	$O + CH_3 \leftrightarrow H + CH_2O$
(R38)	$H + O_2 \leftrightarrow OH + O$
(R45)	$H + HO_2 \leftrightarrow O_2 + H_2$
(R46)	$HO_2 + H \leftrightarrow OH + OH$
(R52)	$H + CH_3 + M \leftrightarrow CH_4 + M$
(R53)	$H + CH_4 \leftrightarrow H_2 + CH_3$
(R58)	$H + CH_2O \leftrightarrow H_2 + HCO$
(R84)	$OH + H_2 \leftrightarrow H + H_2O$
(R97)	$OH + CH_3 \leftrightarrow CH_2(S) + H_2O$
(R98)	$OH + CH_4 \leftrightarrow CH_3 + H_2O$
(R99)	$OH + CO \leftrightarrow H + CO_2$
(R101)	$OH + CH_2O \leftrightarrow HCO + H_2O$
(R166)	$HCO + H_2O \leftrightarrow H + CO + H_2O$
(R167)	$HCO + M \leftrightarrow H + CO + M$
(R168)	$O_2 + HCO \leftrightarrow HO_2 + CO$
(R284)	$O + CH_3 \leftrightarrow H + H_2 + CO$

and (R46) all increase and become comparable to reactions (R53) and (R98). At 64% of CO and 16% of CH_4, the rate of CO oxidation reaction (R99) is comparable to that of H_2 oxidation reaction (R84) and the rate of OH production reaction (R46) is higher than that of methane dehydrogenation reactions (R98) and (R53). When the concentration of CO is increased to 75.2%, the rate of CO oxidation reaction (R99) exceeds that of H_2 and CH_4 reactions. For the case of 20% H_2-78.4% CO-1.6% CH_4 in the fuel mixture, the CH_4 chemistry plays only a minor role in the overall reaction as evident by the rate of reactions (R98) and (R53). At such a condition the CO and H_2 chemistries dominate the entire reaction as those in syngas flame. Fig. 11 shows that when the CO concentration is low (8%), the major contributions to positive heat release are the reactions (R10), (284), and (R84). As the concentration of CO is increased, the reactions (R99) and (R46) not only become more active but also contribute to a significant amount of heat release. And finally the reactions (R99), (R46), and (R84) contribute to almost the entire heat release of the flame as the CO concentration reaches 78.4%.

Comparison of Figs. 10 and 11 reveals that for the stoichiometric H_2/CO/CH_4/air flame with 20% H_2 concentration the rate of reactions (R99) and (R46) and their contributions to heat-release rate all increase with increasing the CO content in the fuel mixture. Recall that the adiabatic flame temperature (Fig. 2) and laminar burning velocity (Fig. 3) are also increased with increasing the CO content in the fuel mixture. This fact suggests that the reactions (R99) and (R46), which have high heat release rate and high reaction rate, play an important role in affecting the heat release behavior and the laminar burning velocity as the CO content in the fuel is varied.

To interpret the influence of chemical reaction effect on laminar burning velocity of the stoichiometric H_2/CO/CH_4/air flame, the results of sensitivity analysis of laminar burning velocity is shown in Fig. 12 for H_2 concentration fixed at 20%. Similar sensitivity analysis is also performed for the case of

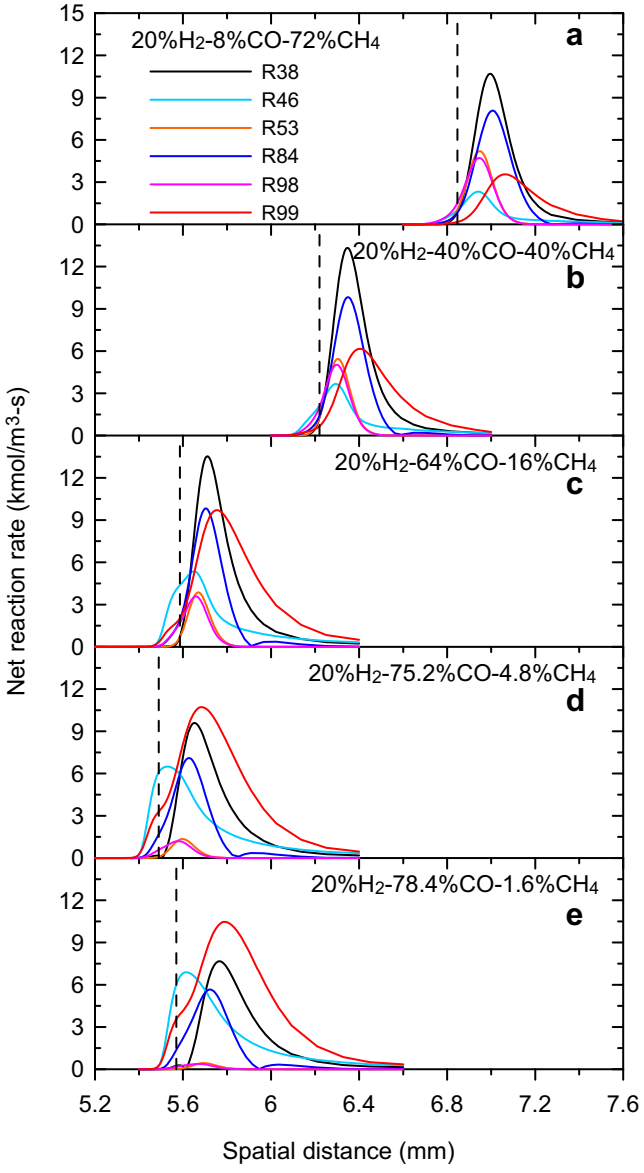

Fig. 10 – Comparison of the net reaction rate for the premixed stoichiometric H_2/CO/CH_4/air flames.

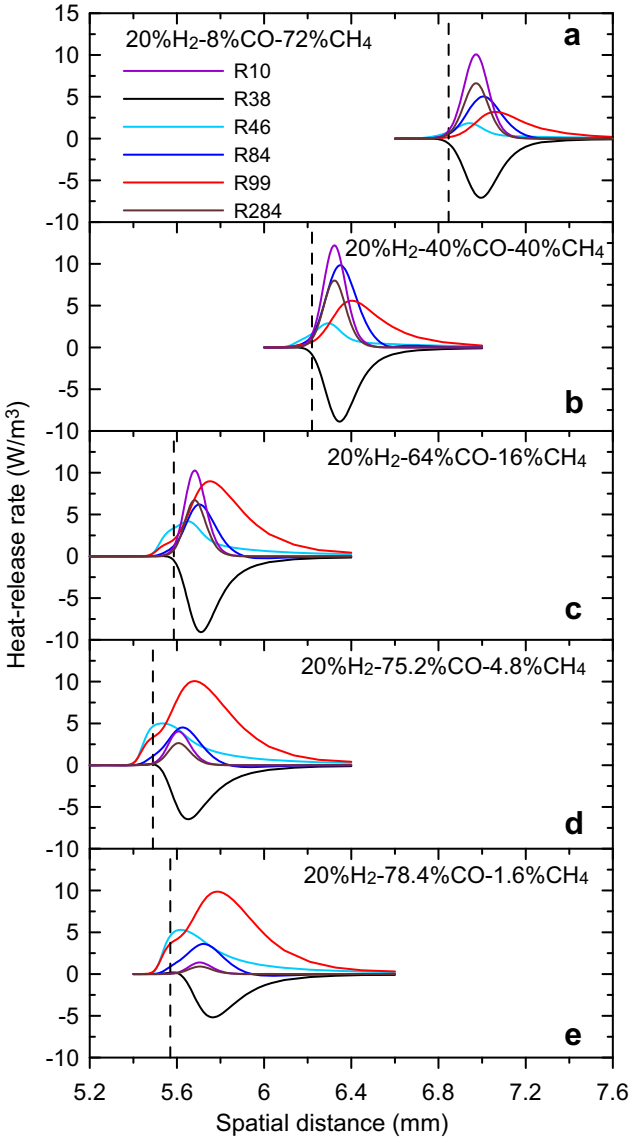

Fig. 11 – Comparison of the heat-release rate for the premixed stoichiometric H_2/CO/CH_4/air flames.

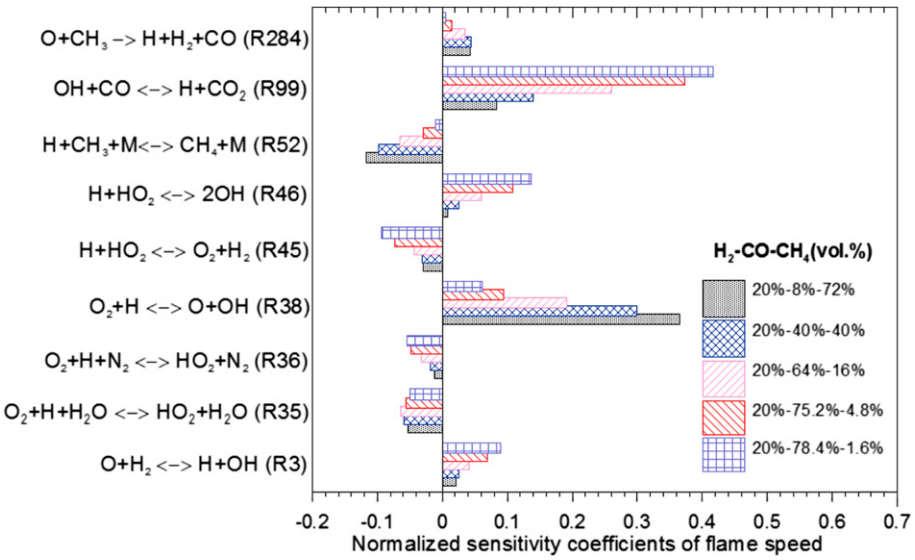

Fig. 12 – Sensitivity analysis of laminar burning velocity for the stoichiometric H_2/CO/CH_4/air flame with 20% of H_2 in the fuel mixture.

10% H_2 in the fuel mixture (not shown here). The trend of the variation of sensitivity coefficients is similar to that shown in Fig. 12. It can be seen that the sensitivities to reaction steps (R38) and (R52) are high when CO concentration is low in the fuel mixture and they become lower as the concentration of CO is increased. The sensitivities to reaction steps (R3), (R45), (R46), and (R99) become higher as the concentration of CO is increased in the fuel mixture and the sensitivities to steps (R46) and (R99) are higher than those of (R3) and (R45). This confirms that the reactions (R99) and (R46) play a dominant role in affecting the laminar burning velocity as the CO content in the fuel is increased.

4. Conclusions

In the present study, the effect of fuel composition variations on the characteristics of H_2/CO/CH_4/air flames is examined systematically. The adiabatic flame temperatures and laminar burning velocities of the premixed *stoichiometric* H_2/CO/CH_4/air flames under various fuel compositions are calculated using the EQUIL and PREMIX codes of Chemkin collection 3.5, respectively. Whereas the flame structures of the laminar premixed stoichiometric H_2/CO/CH_4/air opposed-jet flames are simulated using the OPPDIF package with the GRI-Mech 3.0 full chemical kinetic mechanisms and detailed transport properties. Experimental measurements of the flame front position and temperature of the opposed-jet flames under various fuel compositions are performed and compared to numerical predictions. The main results are summarized as follows:

(1) Computed results show that the addition of H_2 to the CH_4/air flame only has minor effect on adiabatic flame temperature. The addition of CO to the CH_4/air flame has a slightly better effect on flame temperature than that of H_2.

(2) The laminar burning velocity increases with increasing H_2 or CO addition to the CH_4/air flame. When there is no CO in the fuel mixture, the increase of H_2 volumetric fraction from 0% to 50% increases the laminar burning velocity by 50%. However, with 0% of H_2 in the fuel mixture, the increase of CO volumetric fraction from 0% to 50% increases the laminar burning velocity only by 26%. When 10% of H_2 is added to the CO/CH_4 fuel mixture, the laminar burning velocity is increased, especially for the condition of 100% of CO in the CO/CH_4 mixture. The burning velocity has increased from near zero for the pure CO premixed flame to a value of 46 cm/s for the flame with 10% H_2–90% CO-0% CH_4 (100% CO in CO/CH_4) in the fuel mixture. In addition, the increase of H_2 content in the blended fuel not only increases the burning velocity, but also shifts the maximum burning velocity from that occurred at the condition of 10% H_2-81% CO-9% CH_4 (90% CO in CO/CH_4) to 50% H_2-50% CO-0% CH_4 (100% CO in CO/CH_4).

(3) Comparisons of the predicted flame front position and temperature with the measured data indicate that the numerical model can accurately predict the general flame characteristics. This, in turn, validates the correct settings of the boundary conditions in the model and also shows the capability of the GRI-Mech 3.0 mechanisms for H_2/CO/CH_4/air flame calculations.

(4) For a fixed stoichiometry of the H_2/CO/CH_4/air flame with H_2 content ranging from 0% to 20%, the reaction rate of reactions (R38), (R46), and (R84) increases with increasing H_2 content in the fuel mixture. The increase of the rate of reactions (R38) and (R46) enhances active OH radical productions, while the increase of the rate of reaction (R84) accelerates H_2 oxidation. The reactions (R46) and (R84) only release small amount of heat as compared to the other major reactions. These facts suggest that the increase in the laminar flame speed with H_2 addition is most likely due to an increase in active radicals during combustion

(chemical effect), rather than from changes in the adiabatic flame temperature (thermal effect).

(5) For the stoichiometric $H_2/CO/CH_4$/air flame with H_2 concentration fixed at 10% and 20% the rate of reactions (R99) and (R46) and their contributions to heat-release rate are all increased with increasing the CO content in the fuel mixture. This fact suggests that the reactions (R99) and (R46), which have high heat release rate and high reaction rate, play an important role in affecting the heat release behavior and the laminar burning velocity as the CO content in the fuel is varied. Sensitivity analysis confirms that the reactions (R99) and (R46) play a dominant role in affecting the laminar burning velocity as the CO content in the fuel is increased.

Acknowledgments

This research was supported by the National Science Council of Republic of China under Grant number NSC96-2212-E-216-016-MY3.

REFERENCES

[1] Demirbas A. Combustion characteristics of different biomass fuels. Prog Energy Combust Sci 2004;30:219–30.
[2] FAO. Wood gas as engine fuel. Rome: Food and Agricultural Organization of the United Nations (FAO); 1993.
[3] Hanaoka T, Inoue S, Uno S, Ogi T, Minowa T. Effect of woody biomass components on air–steam gasification. Biomass Bioenergy 2005;28:69–76.
[4] Lv P, Yuan Z, Ma L, Wu C, Chen Y, Zhu J. Hydrogen-rich gas production from biomass air and oxygen/steam gasification in a downdraft gasifier. Renewable Energy 2007;32:2173–85.
[5] Yu G, Law CK, Wu CK. Laminar flame speeds of hydrocarbon t air mixtures with hydrogen addition. Combust Flame 1986; 63(3):339–47.
[6] Halter F, Chauveau C, Djebaili-Chaumeix N, Gokalp I. Characterization of the effects of pressure and hydrogen concentration on laminar burning velocities of methane–hydrogen–air mixtures. Proc Combust Inst 2005; 30(1):201–8.
[7] Zhang Y, Wu J, Ishizuka S. Hydrogen addition effect on laminar burning velocity, flame temperature and flame stability of a planar and a curved CH_4–H_2–air premixed flame. Int J Hydrogen Energy 2009;34:519–27.
[8] Wang J, Huang Z, Tang C, Miao H, Wang X. Numerical study of the effect of hydrogen addition on methane–air mixtures combustion. Int J Hydrogen Energy 2009;34:1084–96.
[9] Hu E, Huang Z, He J, Jin C, Zheng J. Experimental and numerical study on laminar burning characteristics of premixed methane–hydrogen–air flames. Int J Hydrogen Energy 2009;34:4876–88.
[10] Huang Z, Zhang Y, Zeng K, Liu B, Wang Q, Jiang D. Measurements of laminar burning velocities for natural gas-hydrogen-air mixtures. Combust Flame 2006;146(1–2): 302–11.
[11] Yan B, Wu Y, Kiu C, Yu JF, Li B, Li ZS, et al. Experimental and modeling study of laminar burning velocity of biomass derived gases/air mixtures. Int J Hydrogen Energy 2011;36: 37692–43777.
[12] Troe J. Modeling the temperature and pressure dependence of the reaction $HO + CO \leftrightarrow H + CO_2$. Proc Combust Inst 1998; 27(1):167–75.
[13] Rightley ML, Williams FA. Burning velocities of CO flames. Combust Flame 1997;110:285–97.
[14] Yetter RA, Dryer FL. Inhibition of moist carbon monoxide oxidation by trace amounts of hydrocarbons. Proc Combust Inst 1992;24:757–67.
[15] Park J, Kim JS, Chung JO, Yun JH, Keel SI. Chemical effects of added CO_2 on the extinction characteristics of $H_2/CO/CO_2$ syngas diffusion flames. Int J Hydrogen Energy 2009;34: 8756–62.
[16] Ouimette P, Seers P. NO_x emission characteristics of partially premixed laminar flames of $H_2/CO/CO_2$ mixtures. Int J Hydrogen Energy 2009;34:9603–10.
[17] Zhang X, Huang Z, Zhang Z, Zheng J, Yu W, Jiang D. Measurements of laminar burning velocities and flame stability analysis for dissociated methanol-air-diluent mixtures at elevated temperatures and pressures. Int J Hydrogen Energy 2009;34(11):4862–75.
[18] Vagelopoulos CM, Egolfopoulos FN. Laminar flame speeds and extinction strain rates of mixtures of carbon monoxide with hydrogen, methane, and air. Proc Combust Inst 1994;25: 1317–23.
[19] Wu CY, Chao YC, Cheng TS, Chen CP, Ho Ct. Effects of CO addition on the characteristics of laminar premixed CH_4/air opposed-jet flames. Combust Flame 2009;156:362–73.
[20] Egolfopoulos FN, Du DX, Law CK. A study on ethanol oxidation kinetics in laminar premixed flames, flow reactors, and shock tubes. Proc Combust Inst 1992;24:833–41.
[21] Huang Y, Sung CJ, Eng JA. Laminar flame speeds of primary reference fuels and reformer gas mixtures. Combust Flame 2004;139:239–51.
[22] Kent JH. A noncatalytic coating for platinum-rhodium thermocouples. Combust Flame 1970;14:279–81.
[23] Becker HA, Yamazaki S. Entrainment, momentum flux and temperature in vertical free turbulent diffusion flames. Combust Flame 1978;33:123–49.
[24] Chao YC, Jeng MS. Behavior of the lifted jet flame under acoustic excitation. Proc Combust Inst 1992;24:333–40.
[25] Smith GP, Golden DM, Frenklach M, Moriarty NW, Eiteneer B, Goldenberg M, et al. GRI-Mech 3.0, <http://www.me.berkeley.edu/gri_mech/>.
[26] Sung CJ, Huang Y, Eng JA. Effects of reformer gas addition on the laminar flame speeds and flammability limits of n-butane and iso-butane flames. Combust Flame 2001;126: 1699–713.